Optical Properties of the Metal ReO_3 from 0.1 to 22 eV

J. FEINLEIB, W. J. SCOULER, AND A. FERRETTI
Lincoln Laboratory, Massachusetts Institute of Technology, Lexington, Massachusetts*
(Received 26 June 1967)

Absolute-reflectance measurements of single-crystal ReO_3 in the spectral range 0.2–22 eV are analyzed by Kramers-Kronig relations to give the real and imaginary parts of the dielectric constants. The dielectric constant is characteristic of free-electron behavior below the sharp plasma edge at 2.1 eV, and confirms the metallic nature of the lustrous red oxide. Interband transitions dominate the optical spectrum above the plasma edge. From our analysis we derive an optical effective mass of $0.86m_0$. The metallic properties and interband transitions are discussed in terms of proposed band models.

I. INTRODUCTION

THE electrical and magnetic behavior of the transition-metal oxides ranges from magnetic insulators, or low-mobility semiconductors, to high-carrier-density, nonmagnetic metals. The common characteristic of these oxides is an incomplete electron d shell of the metal ion, and it is the binding of these electrons, whether localized in transition-metal oxygen complexes, or itinerant in electronic energy bands, that determines the diverse properties of these compounds. These oxides provide the experimental test for the transition between the crystal field and the one-electron band models.[1] Our optical measurements are part of a study of rhenium trioxide ReO_3, which is a member of the transition-metal oxide group that exhibits properties characteristic of a good metallic conductor.[2]

The ReO_3 crystal structure is essentially simple cubic, with rhenium ions at the corners of the cube as shown in Fig. 1. This structure is closely related to perovskites like $SrTiO_3$; the additional Sr ion of that compound occupies the center of the cube. The simple crystal structure reduces band-structure computation considerably, and while little has yet been done on ReO_3, relevant theoretical and experimental studies of $SrTiO_3$ have been made.[3]

The outer electron shell in the rhenium ion has the configuration $5d^5\,6s^2$. In a purely ionic ReO_3 compound of Re^{6+} and O^{2-}, the cation would have one electron remaining in the d shell. Thus, in a one-electron band model, ReO_3 should be metallic, as is found experimentally.[2] The similar oxide of tungsten, with one electron fewer than rhenium, is found to be an insulator in keeping with this band model, and in addition, the sodium tungsten bronzes, Na_xWO_3, where the sodium atom may contribute one electron to the conduction band, are also found to be metallic[4–6] and have an optical spectrum similar to the one which we have measured for ReO_3. Thus, while it is apparent that the band picture is appropriate for these compounds, the controversy over the actual band scheme has yet to be resolved by both theory and experiment. In particular, we can list at least five band schemes which have been proposed to explain the metallic properties of the sodium tungsten bronzes, and their relevance to ReO_3 is easily seen. In the notation of Fromhold and Narath,[7] the band models are labeled according to the atomic wave function believed to form the lowest conduction band; these models are:

(1) Sienko[6] model: tungsten $5d$ (t_{2g}) states;
(2) Keller[8] model: tungsten $6s$ states;
(3) Mackintosh[9] model: sodium $3p$ states;
(4) Fuchs[10] model: sodium states;
(5) Goodenough[2] model: π bonded oxygen and tungsten $5d$ (t_{2g}) states.

Models 3 and 4, which require participation of sodium states in the conduction band, are immediately ruled out as inapplicable to ReO_3, and since the properties of ReO_3 and Na_xWO_3 are so similar, these models would seem to be inapplicable to the bronzes as well. In addition, Fromhold and Narath[7] have argued that the

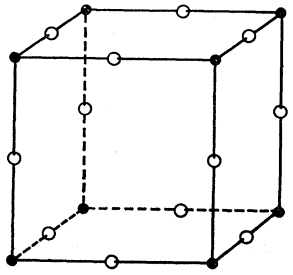

FIG. 1. ReO_3 crystal structure. Open circle, oxygen positions; closed circles, cation sites at cube corners.

* Operated with support from the U. S. Air Force.

[1] F. J. Morin, in *Semiconductors*, edited by N. B. Hannay (Reinhold Publishing Corp., New York, 1959); F. J. Morin, Phys. Rev. Letters **3**, 34 (1959); N. F. Mott, Phil. Mag. **6**, 287 (1961); D. Adler, J. Feinleib, H. Brooks, and W. Paul, Phys. Rev. **155**, 851 (1967); J. B. Goodenough, *Magnetism and the Chemical Bond* (Interscience Publishers, Inc., New York, 1963); J. B. Goodenough, J. Appl. Phys. **37**, 1415 (1966).

[2] A. Ferretti, D. B. Rogers, and J. B. Goodenough, J. Phys. Chem. Solids **26**, 2007 (1965).

[3] A. H. Kahn and A. J. Leyendecker, Phys. Rev. **135**, A1321 (1964); M. Cardona, *ibid.* **140**, A651 (1965).

[4] B. W. Brown and E. Banks, Phys. Rev. **84**, 609 (1951).

[5] H. R. Shanks, P. H. Sidles, and G. C. Danielson, in *Advances in Chemistry*, edited by R. Ward (American Chemical Society, Washington, D. C., 1963), Series 39.

[6] M. J. Sienko, in Ref. 5.

[7] A. T. Fromhold, Jr., and A. Narath, Phys. Rev. **152**, 585 (1966); J. M. Honig and J. O. Dimmock, M.I.T. Lincoln Laboratory Solid-State Research Report No. 1965:3, p. 38 (unpublished).

[8] J. M. Keller, J. Chem. Phys. **33**, 232 (1960).

[9] A. R. Mackintosh, J. Chem. Phys. **38**, 1991 (1963).

[10] R. Fuchs, J. Chem. Phys. **42**, 3781 (1965).

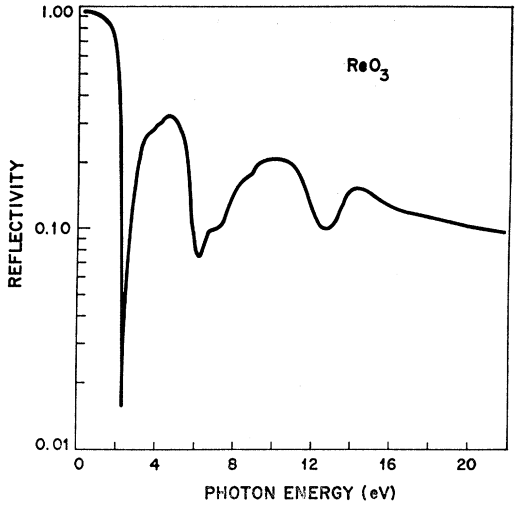

FIG. 2. Reflectivity of ReO_3 versus photon energy.

Knight shifts of the ^{23}Na and ^{183}W nuclear magnetic resonances[11,12] are not consistent with the model of sodium conduction band states. They have also ruled out an *s*-state conduction band, as in model 2.

The remaining models, 1 and 5, both have the desirable capability of describing both ReO_3 and Na_xWO_3. The essential difference between these models is the degree of covalent bonding admitted into the conduction-band wave function, as Sienko[6] has noted. Although this distinction is important in the molecular orbital model and is useful for constructing tight-binding wave functions,[13] a complete band calculation should make these models less distinguishable since the admixture of wave functions changes from one part of **k** space to another. A more relevant consideration, from the point of view of the optical structure, is the separation of the *d* bands and the *s* and *p* bands.

The analysis of our data of the reflectivity of ReO_3 from 0.2 to 22 eV has revealed several features of the band structure of this material and can be used to fix parameters within the framework of these band models.

II. EXPERIMENTAL RESULTS

A. Optical Measurements

Room-temperature reflectance measurements at near normal incidence were made on an "as-grown" face of a 2-mm-cube crystal of ReO_3. The crystal was grown by a vapor-transport technique and shows good stoichiometry.[2] At photon energies from 0.2 to 3.5 eV, the measurements were made using a Perkin-Elmer single-beam prism monochromator in conjunction with a reflectometer designed specifically for absolute measurements of small crystals.[14] Reproducibility and accuracy of the results using this system are of the order of a few tenths of percent, except below 0.8 eV, where the inaccuracy is of the order of 0.5%.

From 3.5 to 22 eV, a McPherson monochromator was used. This experimental arrangement is very similar to that which has been described previously.[15] Since the McPherson monochromator could be used to 2 eV, the data from 2 to 3.5 eV could be normalized to the absolute data obtained with the lower-energy monochromator. The data above 10 eV were taken using He and Ne gases in a hot-filament light source similar to one previously described.[16]

The results of the reflectivity measurements are plotted as the log of the absolute reflectivity versus photon energy in Fig. 2. At the lowest energy, the reflectivity reaches a value of about 93% and then decreases smoothly until the dielectric anomaly, or plasma edge, is reached. The minimum reflectivity reached at room temperature at 2.30 eV is about 1.5%, but preliminary measurements at liquid-helium temperature show a minimum of less than 0.8%. The rise from the minimum is due to the onset of interband transitions which peak about 4 eV. Other reflectivity shoulders and peaks, due to additional electronic transitions, occur around 7, 8, 10, and 14 eV. Beyond this, the reflectivity tails off rather smoothly to 22 eV but is still relatively high, indicating that significant absorption processes are still occurring at higher energies.

B. dc Conductivity

The dc conductivity of our sample was also determined in order to compare the dc value with the optical conductivity, which will be derived in the analysis of our reflectivity data. Because the sample was so small ($\sim 2\times 2\times 1.5$ mm thick), the usual four-probe conductivity measurement was not feasible; therefore, the Van der Pauw[17] technique was used. This consists of making four knife-edge contacts to an odd-shaped sample which has two flat, parallel surfaces. The sample had this configuration and required about 5 A to get measurable voltage readings. Near ambient temperature was maintained by immersing the sample in a liquid bath. The conductivity measured was $\sigma_{dc}=5.5\times 10^4$ $(\Omega\ \text{cm})^{-1}$. As a check on the technique, a similar sized sample of copper was measured and a value of $\sigma_{dc}=5.3\times 10^5$ $(\Omega\ \text{cm})^{-1}$ was obtained. This is within 10% of the handbook value and within 5% of the value measured on a long piece of the same copper sample using the usual four-probe configuration. Thus, we feel reasonably certain that the measured conductivity of our ReO_3 sample is within 25% of the bulk conductivity, allowing for small irregularities in the geometry of the sample.

[11] W. H. Jones, Jr., E. A. Garbaty, and R. G. Barnes, J. Chem. Phys. **36**, 494 (1962).
[12] A. Narath and D. C. Wallace, Phys. Rev. **127**, 724 (1962).
[13] J. M. Honig and J. O. Dimmock, M.I.T. Lincoln Laboratory Solid-State Research Report No. 1965:3, p. 38 (unpublished).
[14] J. Feinleib and B. Feldman, Rev. Sci. Instr. **38**, 32 (1967).
[15] W. J. Scouler, Appl. Opt. **3**, 341 (1964).
[16] P. L. Hartman, J. Opt. Am. **51**, 113 (1961).
[17] L. J. Van der Pauw, Philips Res. Rept. **13**, 1 (1958).

III. COMPLEX DIELECTRIC CONSTANT FOR A METAL

The dc conductivity and reflectivity data are consistent with the behavior of a metal. Therefore, we have analyzed the data in a manner very similar to that used by Ehrenreich and Philipp[18] in their treatment of the data of silver, copper, and aluminum[19]; i.e., the optical properties are due to the effects of both free and bound electrons and the contributions of each to the total dielectric constant can be determined by proper analysis.

As is well known, a Kramers-Kronig (KK) analysis of the reflectivity data R can be used to calculate the optical and dielectric constants which are related as follows:

$$(n-1-ik)/(n+1-ik)=R^{1/2}e^{i\theta}, \tag{1}$$

$$\epsilon=\epsilon_1-i\epsilon_2=(n-ik)^2, \tag{2}$$

$$\epsilon_1=n^2-k^2, \tag{3}$$

$$\epsilon_2=2nk, \tag{4}$$

$$\theta(E_0)=\frac{E_0}{\pi}\int_0^\infty \frac{\ln[R(E)/R(E_0)]dE}{E^2-E_0^2}, \tag{5}$$

where E is the photon energy. By calculating θ and by suitable algebraic manipulations, one can obtain the dielectric constants from the reflectivity data.

However, since R is not known over the entire energy spectrum, it is necessary to extrapolate $R(E)$ to infinite energies, usually by a power law. One can use an extrapolation which will force the optical or dielectric constants to agree with some independent measurement at a particular energy. For example, ellipsometric measurements on metals will yield ϵ_1, ϵ_2 or n, k directly. For dielectrics or semiconductors, we can require $k=0$ below the absorption edge.

Since our data extends to 22 eV, we decomposed the integral in Eq. (5) into an integral using the experimental data from 0 to 22 eV[20] and an integral using $R=CE^{-\beta}$ from 22 eV to infinity. The latter integral can be transformed into

$$(E_0/\pi)\int_{22}^\infty \frac{\ln[R(E)/R(E_0)]dE}{E^2-E_0^2}=-\frac{1}{\pi}\left\{\tfrac{1}{2}\ln\frac{R(22)}{R(E_0)}\times\ln\left[\frac{(22+E_0)}{(22-E_0)}\right]-\beta\sum_{0=l}^{\infty}\frac{1}{(2l+1)^2}\left(\frac{E_0}{22}\right)^{2l+1}\right\}. \tag{6}$$

If an independent measurement of n or k were available for some E_0, we could vary β in order to give us $\theta(E_0)$ and therefore n, k, which would agree with the independent values.

[18] H. Ehrenreich and H. R. Philipp, Phys. Rev. **128**, 1622 (1962).
[19] H. Ehrenreich, H. R. Philipp, and B. Segall, Phys. Rev. **132**, 1918 (1963).
[20] From 0 to 0.2 eV, we used the free-electron model, described later, to compute R.

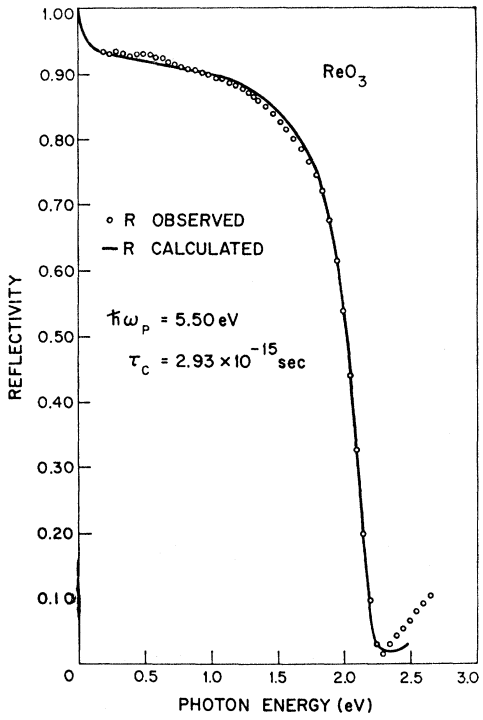

FIG. 3. Comparison of experimental reflectivity with the best fit calculated using Eqs. (9)–(11). In Eq. (9), c has been replaced by $\epsilon_1{}^b(E)$, calculated from Eq. (13).

Such independent n and k values are not available, so we have used the following procedure which is basically a fit of the low-energy data to a modified free-electron model. The total dielectric constant is a sum of free- and bound-electron contributions;

$$\epsilon=\epsilon^f+\epsilon^b, \quad \epsilon^b=\epsilon_1{}^b+i\epsilon_2{}^b. \tag{7}$$

Here $\epsilon_2{}^b$ is a measure of the strength of interband transitions and is zero for energies below the threshold for the first interband transition.

The free-electron model of Drude gives

$$\epsilon^f=1-\omega_p{}^2/\omega(\omega+i/\tau_c), \tag{8}$$

where $\omega_p{}^2=4\pi n_c e^2/m^*$ (plasma frequency), n_c is the conduction electron density, m^* is the effective mass, and τ_c is the relaxation time.

For our analysis, we assumed $\epsilon_2{}^b=0$ for $\hbar\omega=E<E_i=2.30$ eV. This is reasonable, since the reflectivity data below 2.30 eV is smooth and shows no structure characteristic of interband transitions. Preliminary helium-temperature data also show no structure; as a first approximation, we set $\epsilon_1{}^b=c$ (constant). Later we will calculate the actual energy dependence of $\epsilon_1{}^b$ and redo the analysis using $\epsilon_1{}^b(E)$ rather than $\epsilon_1{}^b=c$. From these assumptions, we can write for $E<E_i=2.3$ eV

$$\epsilon_1=\epsilon_1{}^f+c=1-\omega_p{}^2/(\omega^2+1/\tau_c{}^2)+c, \tag{9}$$

$$\epsilon_2=\epsilon_2{}^f=\omega_p{}^2/\omega\tau_c(\omega^2+1/\tau_c{}^2). \tag{10}$$

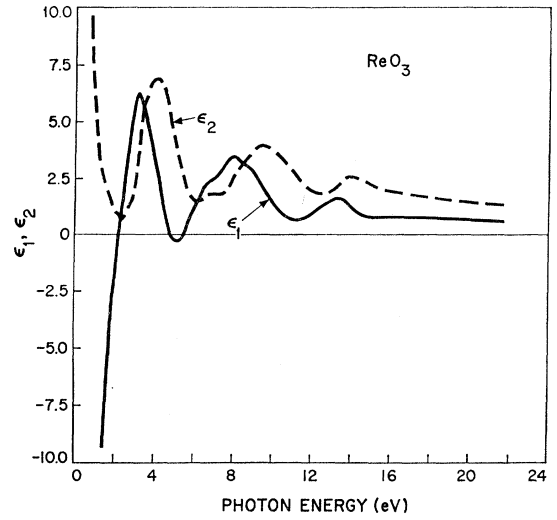

FIG. 4. Real and imaginary parts of the dielectric constant, ϵ_1 and ϵ_2, obtained from the KK analysis.

R is related to ϵ_1 and ϵ_2 by the relation

$$R=\frac{(\epsilon_1^2+\epsilon_2^2)^{1/2}+1-\sqrt{2}[\epsilon_1+(\epsilon_1^2+\epsilon_2^2)^{1/2}]^{1/2}}{(\epsilon_1^2+\epsilon_2^2)^{1/2}+1+\sqrt{2}[\epsilon_1+(\epsilon_1^2+\epsilon_2^2)^{1/2}]^{1/2}}. \quad (11)$$

The parameters ω_p, τ_c, and c were then varied in a least-squares analysis by a computer until a best fit with the measured reflectivity below 2.3 eV was obtained. Using the first best-fit parameters which give ϵ_1, ϵ_2, we calculated θ at 1.0 eV $[\theta_1(1.0)]$.[21] We then did a KK analysis on the complete R spectrum, varying β in Eq. (6) so that the KK value of θ at 1.0 eV agreed with $\theta_1(1.0)$. We also obtained ϵ_1 and ϵ_2.

Having done this, we can now calculate $\epsilon_1{}^b(E)$, which in our first approximation we set equal to a constant c. Since $\epsilon_1(E)$ and $\epsilon_1{}^f(E)$ both satisfy the KK relations, so also does $\epsilon_1{}^b$. We may therefore write

$$\epsilon_1{}^b(E_0)=\frac{2}{\pi}\int_0^\infty \frac{\epsilon_2{}^b(E)EdE}{E^2-E_0{}^2}. \quad (12)$$

However, since $\epsilon_2{}^b$ describes real interband transitions which begin about $E_i=2.3$ eV, we can set $\epsilon_2{}^b=0$ for $E<E_i$ as we did in the least-squares analysis. Above E_i, since $\epsilon_2{}^b=\epsilon_2-\epsilon_2{}^f$, we can subtract $\epsilon_2{}^f$, which is small, from our ϵ_2 deduced from the KK analysis. Thus,

$$\epsilon_1{}^b(E_0)=\frac{2}{\pi}\int_{E_i}^\infty \frac{[\epsilon_2(E)-\epsilon_2{}^f(E)]EdE}{E^2-E_0{}^2}, \quad (13)$$

which can be numerically integrated on the computer.

[21] θ is given by the relation $\theta=\arctan 2k/(1-n^2-k^2)$ and is limited to values $0\geq\theta\geq-\pi$. These limits result from the convention of signs used in Eq. (1). A more precise form [G. B. Wright, Appl. Opt. 4, 366 (1964)] is $(1-n+ik)/(1+n-ik)=R^{1/2}e^{i\theta}$, where θ is also limited to $0\geq\theta\geq-\pi$. However, when $k=0$, $\theta=-\pi$ rather than 0, which is obtained in Eq. (1). $\theta=-\pi$ gives the proper reversal of the E vector on reflection. Equation (5) gives $\theta=0$ for $k=0$, which is consistent with Eq. (1). There is no measurable physical difference in either form since we measure only the square of the reflectance amplitude.

At first glance one might be tempted to use $\epsilon_1{}^b=\epsilon_1-\epsilon_1{}^f$ to obtain $\epsilon_1{}^b$ since we have already calculated ϵ_1 and $\epsilon_1{}^f$. However, at low energies ϵ_1 and $\epsilon_1{}^f$ are both large negative numbers and the error in their difference is of the same order as $\epsilon_1{}^b$. At higher energies, above 5.7 eV, both ϵ_1 and $\epsilon_1{}^f$ are smaller and the error obtained in computing $\epsilon_1-\epsilon_1{}^f$ is small compared to $\epsilon_1{}^b$, so that this is a reasonable method of getting $\epsilon_1{}^b$. Having obtained the energy dependence of $\epsilon_1{}^b$ to a good approximation, we used these new values in Eq. (9) for our best-fit procedure instead of the constant c which we varied with ω_p and τ_c. Figure 3 shows the observed reflectivity and the second calculated best fit for the new parameters $\hbar\omega_p=5.50$ eV, $\tau_c=2.93\times10^{-15}$ sec. In this figure, we show the "raw" data as circles. In Fig. 2 and for the KK analysis, a smooth curve was drawn through the scattered points below 0.8 eV. The apparent structure exhibited by the circles should not be taken seriously here since it is within experimental error, as discussed further in Sec. IV.

We used these best-fit parameters and $\epsilon_1{}^b(E)$ to calculate $\theta_2(1.0)$. The complete KK analysis was done again, varying β in Eq. (6) so that the new KK value of θ at 1.0 eV agreed with $\theta_2(1.0)$. We did not carry this self-consistent procedure any further since the differences in $\theta(1.0)$, ω_p, and τ_c using $\epsilon_1{}^b=c$ or $\epsilon_1{}^b(E)$ were small.

Figure 4 shows ϵ_1 and ϵ_2 obtained in the second KK analysis. ϵ_1 rises from a large negative value passing through zero at 2.18 eV$=E_p'$, the observed plasma energy (not the free-electron plasma energy, $\hbar\omega_p=E_p$ $=5.50$ eV). It peaks at 3.2 eV and decreases to a small negative value near 5 eV. This behavior is similar to that of silver.[18]

The ϵ_2 curve is free-electron-like to 2.3 eV, where interband transitions begin. We notice that ϵ_2 is not zero at 2.3 eV, but is small at that point. Above 2.3 eV the peaks in ϵ_2 are due to interband transitions which are prominent at 4.2, 7.0, 8.5, 9.3, and 14.0 eV. These peaks can be correlated with large joint density of states in the energy-band scheme and provide parameters for a band calculation.

From ϵ_1 and ϵ_2, the energy-loss function $\epsilon_2/(\epsilon_1^2+\epsilon_2^2)$

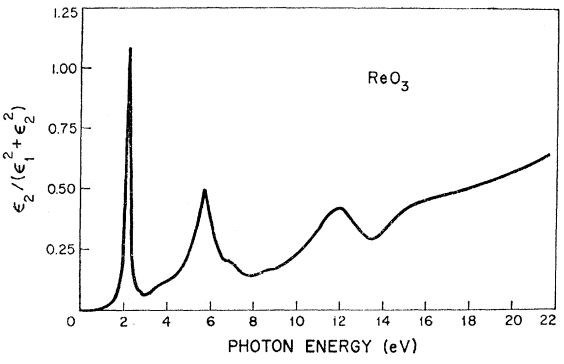

FIG. 5. Loss function.

is calculated and plotted in Fig. 5. The peaks in this curve are due to resonance effects and will be discussed subsequently.

In Fig. 6 we show the results obtained for $\epsilon_1{}^b(E)$ using the $\epsilon_2(E)$ and $\epsilon_2{}^f(E)$ values obtained in the second KK analysis. For $E<5.7$ eV, the KK relation, Eq. (13), was used. Above 5.7 eV, $\epsilon_1{}^b$ was obtained by taking the difference $\epsilon_1-\epsilon_1{}^f$. One important feature of the curve which is pertinent to the discussion of the loss function is that around 5.7 eV, $\epsilon_1{}^b$ is approximately zero at the same point $\epsilon_1{}^f=0$. $\epsilon_1{}^f$ is plotted from our best-fit parameters of Fig. 3 and is shown along with ϵ_1.

In order to demonstrate the value of our approach to the analysis and separation of the free- and bound-electron effects, we show in Fig. 7 plots of the quantities $1-\epsilon_1{}^f$ and $1-\epsilon_1$ (expt)$+\epsilon_1{}^b$ as well as $\epsilon_2{}^f$ and ϵ_2(expt). If the data analysis were entirely accurate the curves would coincide. Over most of the energy range of validity, i.e., $E<2.3$ eV, the curves agree fairly well.

Another quantity of interest which can be obtained in this analysis is n_{eff}, the effective number of electrons per ReO_3 molecule contributing to the optical properties. This is calculated from the oscillator-strength sum rule of the form

$$n_{\text{eff}}(E')=\frac{m_0}{2\pi^2\hbar^2Ne^2}\int_0^{E'}E\epsilon_2(E)dE, \qquad (14)$$

where m_0 is the free electron mass and N is the number of ReO_3 molecules/cc; it is plotted in Fig. 8. As in the case of silver,[18] n_{eff} saturates at about the free-electron value of 1 until the threshold for interband transitions is reached. Below the onset of interband transitions, n_{eff} should agree with the value obtained from

$$\omega_p{}^2=\frac{4\pi n_c e^2}{m^*}=\frac{4\pi n_{\text{eff}}Ne^2}{m_0}. \qquad (15)$$

Since $\hbar\omega_p=E_p=5.50$ eV, we get $n_{\text{eff}}=1.16$, which agrees well with Fig. 8. If we assume one conduction

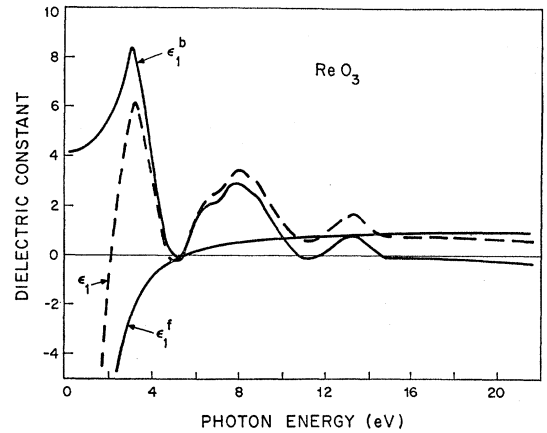

FIG. 6. ϵ_1 obtained from the KK analysis of the reflectivity data, $\epsilon_1{}^b$ calculated from Eq. (13), and $\epsilon_1{}^f$ calculated from Eq. (8) using the best-fit parameters of Fig. 3. Above 5.7 eV, $\epsilon_1{}^b=\epsilon_1-\epsilon_1{}^f$.

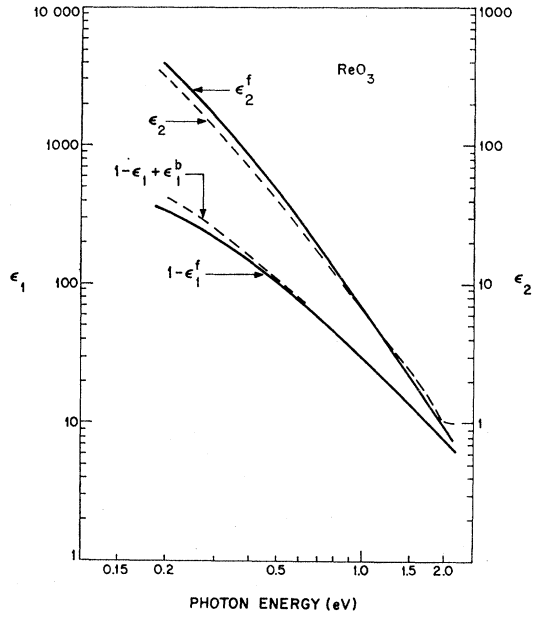

FIG. 7. Comparison of ϵ_2 from the KK analysis, with $\epsilon_2{}^f$ from Eq. (10) using the best-fit parameters of Fig. 3; also, comparison of $1-\epsilon_1+\epsilon_1{}^b$ obtained from the KK analysis with $1-\epsilon_1{}^f$ from Eq. (8).

electron per ReO_3 molecule we get $m^*=0.86m_0$, the optical effective mass.

Above the threshold for interband transitions, n_{eff} rises to another plateau and then increases monotonically to a value of 13 at 22 eV. If we had exhausted all the valence electrons of the Re atom (7) and the three oxygen atoms (18), n_{eff} should saturate again at 25, provided that deeper lying levels are not being excited. Our data do not extend far enough to show this. Since only half of the valence electrons have been involved up to 22 eV, it is not surprising that the reflectivity is still rather high at that point.

IV. DISCUSSION

A. Free-Electron Region

The conductivity value for ReO_3 of $\sigma_{dc}=5.5\times10^4$ $(\Omega\text{ cm})^{-1}$ is typical of a metallic conductor. Although it is nearly a factor of 10 smaller than copper at room temperature, it is roughly the same as the values for transition metals such as Ti or Cr. Therefore, we expect the low-energy optical spectrum to exhibit characteristic free-electron behavior. However, the region of free-electron behavior is limited by the onset of interband transitions. The threshold for interband transitions is an important parameter for band calculations and therefore an accurate determination of the limit of the free-electron region is necessary.

In our analysis, we have determined a best Drude fit to the measured data for energies below 2.3 eV, using Eqs. (9) and (10), and assuming a constant relaxation time τ_c. The extent to which this is a good approxi-

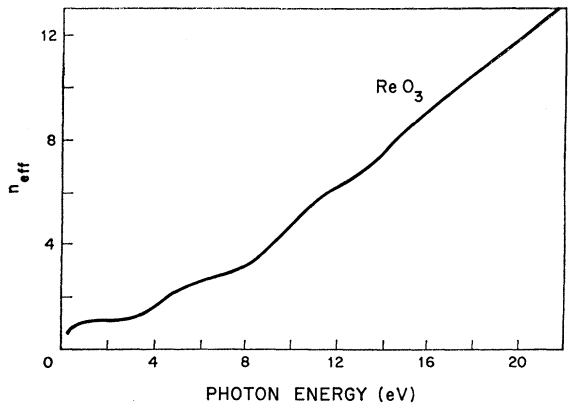

FIG. 8. n_{eff} calculated from the oscillator strength sum rule, Eq. (14).

mation is seen in Fig. 3. The reflectivity calculated from the best-fit Drude curve (which takes into account the screening effects of the higher-energy interband transitions by the self-consistent procedure described) is shown along with the experimental data in this region. There is clearly a close fit within the experimental accuracy except possibly at the lowest photon energies. Below about 0.8 eV, a thermocouple detector was used, and in addition to its inherent low sensitivity and high noise characteristics, the small area of the junction made the measurements extremely sensitive to sample positioning. Thus, we expect the lowest accuracy in absolute reflectivity in this range, probably $\sim 0.5\%$. The maximum deviation of $(R_{obs}-R_{calc})/R_{obs}=1.5\%$ occurs at 0.5 eV. The scatter in the "raw" data of Fig. 3 at low energies would also show up as noticeable structure in the dielectric constants. Since we do not believe that the data are accurate enough to resolve such apparent structure within the scatter, we have smoothed the data for the KK analysis as in Fig. 2 and will not use the data of Fig. 3 to speculate on the possibility of low-energy structure.

Although we can get a good fit with the R curve from the Drude ϵ_1 and ϵ_2, this does not necessarily guarantee good agreement with the dielectric constant calculated from the KK analysis. The agreement between the Drude curve and the latter is seen in Fig. 7, where the real and imaginary parts of the dielectric constant are plotted from the KK data and from the Drude equations (9) and (10). Again the largest deviation occurs at low energies as in the reflectivity fit. Our experiences with the KK analysis has shown that a small error of about 0.5% in the reflectivity at low energies, where R is high, can give an error of 15% or higher in ϵ_1 and/or ϵ_2. Therefore, the separation of the curves does not seem unreasonable in view of the data scatter and approximations used in the analysis.

The relaxation time which enters Eq. (8) would be equal to the dc conductivity scattering time if τ_c were frequency-independent and if the Drude formula were an appropriate approximation over the fitted portion of the spectrum. Using the relation

$$\sigma_{dc}=\frac{ne^2\tau_{dc}}{m^*}=\frac{\omega_p^2\tau_{dc}}{4\pi}, \tag{16}$$

we calculate τ_{dc} to be 8.9×10^{-15} sec compared to the optical relaxation time of $\tau_c=2.9\times10^{-15}$ sec. Thus, the optical relaxation time and conductivity appear to be about $\frac{1}{3}$ of the corresponding dc quantities. We can suggest several reasons for the discrepancy: (1) The measured dc conductivity may be in error by about 25%, as previously mentioned; (2) the surface of the ReO_3 sample used may not be characteristic of the bulk because of contamination or oxidation which gives an error in the measured reflectivity; (3) the relaxation time is not independent of frequency, and as for silver and copper,[18] should be higher at low frequencies than at the high photon frequencies; (4) the Drude fitting is incorrect because unresolved interband transitions come in at energies lower than 2.1 eV. Without any further experimental evidence we believe that the first three arguments could easily account for the discrepancy without resort to the fourth. We have made a careful search over the spectrum below 2.1 eV and have found no evidence for structure in this region. The reflectivity curve follows the same smooth, Drude shape found in the spectrum of silver[18] right up to the sharp minimum which characterizes the onset of the first interband transition in silver. Even weak interband transitions below 2.1 eV would increase ϵ_2 sufficiently so that no sharp minimum would appear in the reflectivity; the spectrum would then have an appearance similar to that of copper as opposed to silver.

The most likely cause for the discrepancy is the assumption of a frequency-independent scattering time in the Drude formulation. Our method for obtaining τ_c was to obtain a best Drude fit to the reflectivity, assuming that τ_c is a frequency independent parameter. First we note that $1/\tau_c^2$ of Eq. (9) is much smaller than ω^2 in most of the frequency range of the curve fitting. Thus, it is not unlikely that a best fit could be achieved with a poor choice of τ_c. Secondly, it has been demonstrated experimentally in copper and silver, for example, that τ_c has a considerable frequency dependence in the range from about 0 to 2 eV, where we have done most of the curve fitting. The τ_c for these latter metals decreases by more than a factor of 2 from the dc to the optical-frequency values. Thus, in addition to the error caused by fitting the curve with a constant τ_c, we should also expect this τ_c to be smaller than τ_{dc} if ReO_3 is to follow the normal behavior. Physically this is expected because the electrons excited by high-energy photons have a much larger density of states to scatter into than the electrons excited by dc fields. We thus conclude that the factor-of-3 discrepancy in our measurements seems quite reasonable and we therefore expect that at most only very weak interband transitions may be possible

below 2.1 eV to interfere with the otherwise free-electron behavior.

B. Plasma Edge

Collective electron effects in the spectrum are notable by the sharp minimum in reflectivity near 2.3 eV as seen in Figs. 2 and 3. A comparison of the spectrum of ReO_3 with that of silver shows that the plasma edge regions of both materials are very similar although the minimum in ReO_3 is at a lower energy than the 3.9 eV minimum in silver. In fact it is the sharp decrease in reflectivity in the green region that accounts for the lustrous red appearance of ReO_3, whereas a less pronounced decrease in reflectivity would give it the color of copper. This decrease in reflectivity shows the characteristics of a transverse plasma oscillation where $\epsilon(E)=0$. From Fig. 4, it is seen that ϵ_2 has decreased to a small value at the plasma edge energy E_p', and ϵ_1 crosses the axis near E_p'. This behavior gives rise to a sharp peak in the loss function $\epsilon_2/(\epsilon_1^2+\epsilon_2^2)$, as seen in Fig. 5. This behavior of the loss function also occurs in silver and has been termed a hybrid resonance by Ehrenreich and Philipp[18] because it depends on the interaction of lower-lying bands with the conduction electrons. This can be seen by referring to Figs. 4 and 6. The bound-electron resonance or interband transition which is indicated by the peak in ϵ_2 in the 3–4 eV region causes a large positive contribution $\epsilon_1{}^b$ to ϵ_1 which forces ϵ_1 through zero before the free-electron plasma energy $E_p=5.5$ eV. The interaction of the bound and free electrons shift the observed plasma energy where $\epsilon_1=0$ to 2.1 eV. At this energy, ϵ_2, and therefore the damping, is so small that a distinct resonance occurs, giving rise to the peak in the loss function.

In Ag the interband transition is only 0.1 eV away from $E_{p'}$, but in ReO_3 it appears to be about 0.8 eV higher in energy. The resonance of the conduction electron alone appears as a peak in the loss function near 5.5 eV. It is probably coincidental that there is no shift from the calculated E_p, for, as seen in Fig. 6, $\epsilon_1{}^b$ is close to zero when $\epsilon_1{}^f$ crosses the axis. The loss-function curve also shows a distinct peak near 12 eV, but while this may indicate a third plasma resonance involving the total density of conduction and lower band electrons, this broad shape may also be indicative of an interband critical-point transition.

C. Interband Transitions

While one would normally make assignments of structure in reflectivity spectra with a known band calculation, we must depart from the procedure in this instance and try to piece together a possible band structure for ReO_3 from our data. Although the crystal structure of this material is simple cubic, a first-principles calculation would be complicated by the ionic nature of the compound and by the treatment of the all important d electrons in the heavy metal. Spin-orbit and relativistic effects should therefore play a strong role in the band calculation. Nevertheless, it should be useful to compare a plausible ReO_3 band structure with related oxide band structures, such as $SrTiO_3$.[3]

The most important consideration in the structure of this metallic oxide is to determine which states comprise the partly filled conduction band. One possibility is a strong covalent interaction between the metal and oxygen ions in which the valence bands are bonding oxygen $2p$ bands and rhenium $6s$ and $5d$ bands, and where the conduction band arises from the overlapping antibonding bands. This would not seem to be a likely picture for metal oxides because of the large chemical difference between the component ions. In addition, the tungsten oxide analogous to ReO_3 is an insulator with an energy gap of $\sim$3 eV.[22] Measurements have been made of the electrical conductivity and Hall effect on the pure[23] and doped tungsten oxides,[5] M_xWO_3, where x is the concentration of univalent metal ion (Na,Li). The measurements of crystals with $x>0.25$, which have the same structure as ReO_3, have shown that the electron concentration is proportional to x, so that one electron is added for each added Na atom. These added electrons are responsible for the metallic behavior in Na_xWO_3 and, it is therefore expected by analogy that the extra d electron of rhenium will occupy the conduction band which will then have an electron density of one per ReO_3 molecule.

The optical data make this picture plausible. From the Drude fit of Eqs. (9) and (10), we were able to determine the plasma frequency for the conduction electrons. Equation (15) relates the plasma frequency to the electron concentration and effective mass, but it is not possible to separate the latter two quantities solely from the reflectivity and conductivity measurements. However, when we assume that each rhenium ion contributes only one electron to the conduction band and that the oxygen anions contribute none, we calculate from Eq. (15) an effective mass of $m^*=0.86m_0$. In addition, with these assumptions, the effective number of electrons in the free-electron region as calculated in the KK analysis, and shown in Fig. 8, saturates at about 1.16, which also agrees with this effective mass.

The effective mass of Na_xWO_3 determined from transport,[5,23] magnetic susceptibility,[24,25] and specific-heat measurements[26] vary from a value below 1 m_0 to about 3 m_0, depending on x and on the sample. The wide variation, as well as the fact that we are comparing a

[22] T. Iwai, J. Phys. Soc. Japan **15**, 1596 (1960).

[23] B. L. Crowder and M. J. Sienko, J. Chem. Phys. **38**, 1576 (1963).

[24] M. J. Sienko and T. B. N. Truong, J. Am. Chem. Soc. **83**, 3939 (1961).

[25] J. D. Greiner, H. R. Shanks, and D. C. Wallace, J. Chem. Phys. **36**, 772 (1962).

[26] R. W. Vest, M. Griffel, and J. F. Smith, J. Chem. Phys. **28**, 293 (1958).

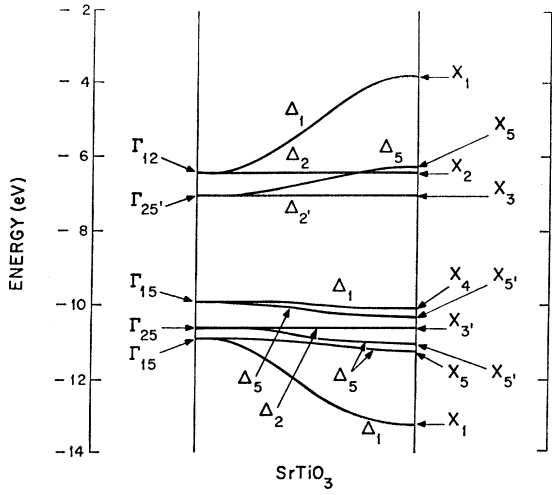

FIG. 9. Energy band structure of $SrTiO_3$ from Ref. 3.

density-of-states effective mass to an optical effective mass, makes it difficult to establish an appropriate value for ReO_3. However, these masses, generally below 2 m_0, are still much lower than would be expected if the conduction band were a narrow d band. For this reason, several of the band models proposed to describe the sodium tungsten bronzes, as described in the Introduction, included the 6s levels or Na s or p levels in the conduction band. While we can readily eliminate the Na contribution on the basis of the analogy with ReO_3, a distinction between s and d band models requires other data. These data have been provided to some extent by the Knight-shift measurements in Na_xWO_3.[7,11,12]

The ^{183}W nuclear resonance was found to have a fast spin-lattice relaxation rate[7] which Fromhold and Narath believe demonstrates that the conduction electrons provide as effective a relaxation mechanism for tungsten nuclei as they do in a similar metal. Therefore, they believe that the tungsten states constitute a major part of the conduction band at the Fermi level. Furthermore, the Knight shift of ^{183}W in $NaWO_3$ was found to be large and negative compared to the large positive shifts in tungsten metal.[27] This implies that there is a low density of s states at the Fermi level, so that the conduction band is composed predominantly of 5d states in a tight-binding description. The other data we have mentioned, magnetic susceptibility and transport, have shown that the width of this d conduction band is probably of the same order as in tungsten metal, and implies a similarly wide d conduction band in ReO_3.

An examination of the absorption data of Brown and Banks[28] for several Na_xWO_3 samples shows that an absorption peak occurs near 2.5 eV. We have made preliminary reflection measurements on Na_xWO_3 single crystals for several different x values and find that the observed plasma edge E_p' increases with x but does not exceed 2.5 eV, in the same manner as the absorption data. We believe that this result is similar to the behavior in ReO_3: the plasma edge is "pinned" to the first interband transition near 3 eV. The interband transition threshold in ReO_3 gives rise to a large absorption peak out to 5 eV as seen from the ϵ_2 curve of Fig. 4. This transition may be either from lower-lying bands to the Fermi level or from the Fermi surface to higher conduction bands, or both. Here we must rely on an educated guess of the band structure to distinguish between these.

D. Band Structure

For this purpose we make use of the energy band calculation of Kahn and Leyendecker[3] of strontium titanate. $SrTiO_3$ has the same crystal structure as ReO_3, except that the strontium ion occupies the center of the unit cell of Fig. 1. In their calculation they have neglected the Sr ion orbitals which lie about 15 eV above the Ti-d bands, so that their calculation may approximate that for a ReO_3 crystal. We need not examine the details of the energy bands, but shall make use of the general result. Firstly, since the metallic oxides show many ionic characteristics, a tight binding, linear combination of atomic orbitals (LCAO) approach seems reasonable. That this is not entirely correct for ReO_3 may be seen from the metallic behavior of the oxide, and from the large oxygen-rhenium overlap integrals estimated by Morin.[29] The separation between oxygen 2p bands and titanium 3d bands is shown to be extremely sensitive to the ionicity in $SrTiO_3$. In fact, an ionicity of 85% of the full ionic charge of the oxygens is sufficient to reduce this splitting from the order of 15 eV to about 3 eV. Thus a similar effect in ReO_3 could cause the 2p to 5d splitting to be reduced further and possibly overlap. Again, however, the evidence of a gap in WO_3 and other rhenium oxides is against this explanation for the metallic behavior, and we estimate from the gap in WO_3 that this splitting may also be of the order of 3 eV. The effect of the Sr ion in the $SrTiO_3$ calculation is shown to be negligible, so that the calculation which concerns only the oxygen 2p and titanium 3d orbitals should be analogous to the bands in ReO_3, where only oxygen 2p and rhenium 5d orbitals are considered.

With this simplified model in mind we have depicted in Fig. 9 the energy band structure of $SrTiO_3$ calculated in Ref. 3, for the Δ axis (100 axis) of the simple cubic Brillouin-zone band structure. Other symmetry directions are given in the reference, but this part is sufficient for our present needs. As shown, the bands labeled Γ_{15},

[27] A. Narath and A. T. Fromhold, Jr., Phys. Rev. 139, A794 (1965).
[28] B. W. Brown and E. Banks, J. Am. Chem. Soc. 76, 963 (1954).
[29] F. J. Morin, in *Proceedings of the International Conference on Semiconductor Physics, Prague, 1960* (Academic Press Inc., New York, 1961), p. 858.

Γ_{25}, and Γ_{15} at the center of the zone, $k=0$, are composed mostly of oxygen $2p$ orbitals from the three oxygen ions per unit cell. The bands labeled $\Gamma_{25'}$ and Γ_{12} are the conduction bands, and are primarily d bands of the metal cation. The symmetry of $\Gamma_{25'}$ is the same as that of the t_{2g} cation orbitals and is therefore triply degenerate at $k=0$; similarly, Γ_{12} has e_g symmetry and is doubly degenerate (orbital degeneracy). In this picture, the valence bands are separated from the d bands by about 3 eV.

For ReO_3, with one electron in the conduction band, the Fermi level lies within the $\Gamma_{25'}$ manifold in this model. The problem, therefore, is to see if the observed optical transition can be accounted for in this situation. As shown, the model is not adequate because a Fermi level in these bands will permit transitions within the bands, from the $\Delta_{2'}$ to Δ_5 starting at very low energies and continuing up until the higher Γ_{12} become involved. Within our experimental error, the optical data show no such low-energy absorptions and it is unlikely that a sharp plasma edge as observed could be obtained even if such transitions were weakened by symmetry and parity selection rules. It appears that the first modification needed is a repositioning of the Fermi level so that the first possible direct transition is of the order of 2 eV.

In the Ti compound for which the bands were calculated, the effect of spin-orbit interaction is small since the atomic spin-orbit splitting[30] is less than 0.1 eV. For the heavy Re cation, this number is much larger, about 1.2 eV, and is not a negligible effect relative to the band splittings.

We have made a preliminary attempt at a parametrized calculation of the effect on the t_{2g} manifold, including the spin-orbit interaction. The method used is the first-order Fourier expansion of the energy bands described by Dresselhaus and Dresselhaus.[31] The procedure allows us to vary the bandwidths relative to the spin-orbit coupling, and the Fermi level at each state is computed by a Monte Carlo procedure which samples **k** space. The details of the procedure and the calculation are outlined in the Appendix.

What we hope to learn from such a calculation is whether or not spin-orbit interactions and a larger bandwidth will change the t_{2g} manifold and Fermi level enough so that interband transitions begin only at above 2 eV. Figure 10 shows an example of the results of such a calculation. The two Fourier parameters are chosen to bring the conduction-band minima to the X point (the face of the Brillouin-zone cube) which is the minima in $SrTiO_3$.[3] The width of the bands is also determined by an arbitrary choice of the parameters

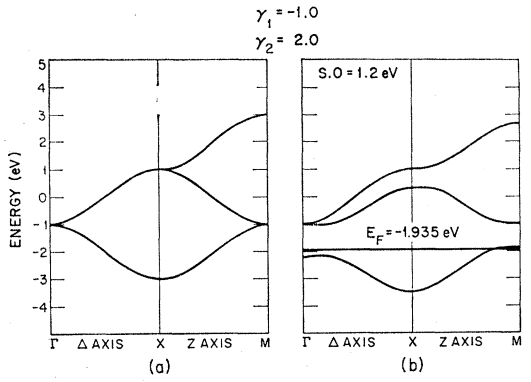

FIG. 10. Preliminary model of bands around Fermi level for ReO_3 (a) without and (b) with spin-orbit interaction.

$\gamma_1 = -1.0$ and $\gamma_2 = 2.0$. Figure 10(a) shows the t_{2g} bands for this choice of parameters with no spin-orbit interaction for two directions in **k** space: the Δ axis goes from the center of the zone to the cube face, and the Z axis goes from the center of the cube face to a cube edge. Figure 10(b) shows the effect of spin-orbit interaction, and includes the calculated Fermi level. The spin-orbit parameter was here taken as 1.2 eV. The full calculation shows that the lowest possible direct transition between d bands, $E_{\min}$, occurs near M with an energy of about 1.1 eV. The strength of such a transition is not determined.

In this highly restricted scheme, $E_{\min}$ cannot be increased beyond 1.2 eV unless the spin-orbit splitting is increased from the atomic value. Since little is known of the true spin-orbit value in crystals of the heavy metal compound, it is possible that we need go no further to explain the free-electron behavior below 2 eV, i.e., the spin-orbit parameter may be larger than that assumed here. Wider d bands will tend to increase the agreement and are in fact necessary to explain the nearly free-electron mass which we calculate from the plasma frequency. The $5d$ bands of rhenium are expected to be significantly wider than $3d$ bands of the Ti compounds because the d character of the bands, which is strongest near the cores, is highly screened for the outer shells, and these bands therefore are more free-electron-like. The lowest interband transition appears to occur within the d bands, from Fermi level to d band, but the interband transitions from lower oxygen bands to the Fermi level probably begin near 3 eV and give rise to the peak in ϵ_2. Some of the other prominent higher-energy transitions should also originate from the oxygen bands, but we require a more definitive band calculation if useful assignments are to be made. These intuitive arguments are no substitute for a careful energy band calculation, but taken with the optical data, we can expect that such calculations should find some interesting changes in the behavior of the d electrons in the series of transition metal oxides in which the outer d shell goes from $3d$ to $5d$.

[30] F. Herman and S. Skillman, *Atomic Structure Calculations* (Prentice-Hall, Inc., Englewood Cliffs, N. J., 1963).

[31] G. Dresselhaus and M. S. Dresselhaus, in *The Optical Properties of Solids*, edited by J. Tauc (Academic Press Inc., New York, 1966), p. 198.

V. CONCLUSION

From our optical measurements and analysis, we have been able to separate the free-electron and interband transition regions of the metal ReO_3 in a manner similar to that of silver.[18] We deduce an optical effective mass of 0.86 m_0 and an interband threshold of about 2 eV. The optical, electrical,[2] and nuclear-resonance data[7,11,12] are consistent with the model of one electron in a rather wide d conduction band. Preliminary band-structure calculations indicate that the first interband transition occurs from the Fermi level to a higher conduction band which is split off due to spin-orbit interaction. Atomic values[30] indicate that this splitting should be about 1.2 eV, while our data suggest 2 eV. However, in view of the approximations made in our calculation of the conduction-band structure, our results seem quite reasonable.

ACKNOWLEDGMENTS

The authors wish to thank Dr. George B. Wright and Dr. Gene Dresselhaus for their help and encouragement. We are also grateful to Bernard Feldman and Eri Cohen for their assistance with the measurements and computer programming, respectively.

APPENDIX

For the ReO_3 crystal, which has a simple cubic Brillouin zone, we have restricted the calculation to the model suggested by the experimental results and by the band calculation of $SrTiO_3$. In this model the predominant band types near the Fermi level are the $5d$ bands, and we assume as shown in Fig. 9 that the oxygen bands are well separated from the d bands. Since direct d orbital overlap is small because of the wide spacing between Re ions, the bandwidth of the $5d$ bands depends on the oxygen overlap. We take this oxygen interaction into account only through an adjustable parameter which determines the bandwidths, as will be described. The problem then reduces to the form

$$H_0\psi=E\psi,$$

where ψ has the e_g and t_{2g} symmetry basis functions at the zone center, so that H_0 is

$$H_0=\begin{array}{c|cc} & e_g & t_{2g} \\ \Gamma_{12} & D_2 & D_{\text{int}} \\ \Gamma_{25'} & D_{\text{int}} & D_3 \end{array}.$$

This problem is further simplified by considering only the lowest set of d bands, the triply degenerate t_{2g} set D_3. Then D_3 has the basis set with symmetry yz, zx, and xy. Putting in the spin function, the zero-order Hamiltonian is

$$H_0=\begin{vmatrix} D_3 & 0 \\ 0 & D_3 \end{vmatrix}, \quad D_3=\begin{vmatrix} h_{11} & 0 & 0 \\ 0 & h_{11} & 0 \\ 0 & 0 & h_{33} \end{vmatrix}.$$

We then need to diagonalize this set so that the spin-orbit interaction may be included; thus,

$$\begin{aligned} \psi&=U\phi, \\ H_0U^{-1}\psi&=EU^{-1}\psi, \\ (UH_0U^{-1})\psi&=E\psi, \\ H_{0'}&=UH_0U^{-1}, \\ (H_{0'}+H_{s.o.})\psi&=E\psi. \end{aligned}$$

The unitary matrix U required for this diagonalization is obtained from Ref. 32.

The method used for determining the matrix elements of the Hamiltonian is the Fourier expansion of the energy-bands procedure of Dresselhaus and Dresselhaus.[31] In this method, since the energy is a periodic function of $\mathbf{k}$ the energy is expanded as

$$E_n(\mathbf{k})=\sum_{\mathbf{d}}\epsilon_n(\mathbf{d})e^{i\mathbf{k}\cdot\mathbf{d}},$$

where $\mathbf{d}$ are real lattice vectors. The Fourier coefficients needed in the expansion are related to band parameters which may be determined experimentally, or, as in our case, they are left as adjustable parameters. The technique is useful when the convergence is rapid, which is found to be true for Ge and Si. We have therefore kept only the first two terms, leaving only two parameters. Thus,

$$\begin{aligned} h_{11}&=\gamma_1(2+\cos ak_z)+\gamma_2, \\ h_{33}&=\gamma_1(2+\cos ak_z)+\gamma_2\cos ak_z. \end{aligned}$$

A computer was then used to solve for $E_n(\mathbf{k})$ along six principal directions. We also used the computer to solve for $E_n(\mathbf{k})$ for the lowest band at a general point in $\mathbf{k}$ space selected by a Monte Carlo procedure. By filling this band with one electron per Re ion, we were then able to determine the Fermi level and band separation for various bandwidths (γ_1/γ_2) and spin-orbit parameter.

[32] G. F. Koster, J. O. Dimmock, and H. Statz, *Properties of Thirty-Two Points Groups* (M.I.T. Press, Cambridge, Mass., 1963).